Tailor-made synthesis of poly(3-hexylthiophene) with carboxylic end groups and its application as a polymer sensitizer in solid-state dye-sensitized solar cells

Ruth Helga Lohwasser,[a] Jayasundera Bandara[ab] and Mukundan Thelakkat*[a]

Received 15th January 2009, Accepted 3rd April 2009
First published as an Advance Article on the web 8th May 2009
DOI: 10.1039/b900921c

We report the first synthesis of regioregular poly(3-hexylthiophene) with carboxylic end groups (P3HT–COOH), show its potential to anchor onto mesoporous TiO_2 and show its application as a polymer sensitizer in a solid-state dye-sensitized solar cell. The incorporation of COOH groups was done by a polymer analogous reaction on P3HT. The product is characterized in comparison with P3HT and low molecular weight model molecules of substituted thiophene. These model compounds are efficient tools to identify end groups in P3HT and P3HT–COOH. The solar cell with 2,2′,7,7′-tetrakis-(*N*,*N*-di-4-methoxyphenylamino)-9,9′-spiro-bifluorene (spiro-OMeTAD) as a hole conductor and P3HT–COOH as a polymer sensitizer on mesoporous TiO_2 shows a short-circuit current of 3.7 mA cm^{-2}, an open circuit voltage of 0.54 V and a power conversion efficiency of 0.9%.

Introduction

Dye-sensitized solar cells are one of the most promising alternatives to conventional photovoltaics. The highest reported efficiencies for cells with liquid I/I_3^- electrolytes and polypyridyl Ru(II)-sensitizers are around 11%.[1] Despite these good performances they still haven't found commercial application due to sealing and long term stability issues.[2] From the point of view of cost reduction and commercialization, alternatives to expensive Ru-dyes and inconvenient liquid electrolytes are necessary. Initial success in solving these problems has already been shown by replacing the liquid electrolyte with a solid hole conductor and by using organic dyes.[3–7] Recently conjugated polymers were reported as polymer sensitizers that are inexpensive alternatives to the standard Ru-dyes.[8–11] Poly(3-hexylthiophene) (P3HT) is a good candidate due to its high charge carrier mobility of up to 0.1 $cm^2 V^{-1} s^{-1}$.[12] Poly(3-alkylthiophenes) with carboxylic groups in the alkyl side chain have already been reported. Many attempts have also been made to introduce new end groups to poly(3-alkylthiophenes) to widen their application and allow end group-driven self-assembly onto surfaces.[13–15]

Here we report the first synthesis of highly regioregular P3HT with carboxylic acid end groups, show its potential to anchor onto mesoporous TiO_2 and show its use as a polymer sensitizer in a solid-state dye-sensitized solar cell.

Results and discussion

Synthesis and characterization

The COOH end groups were introduced by a polymer analogous functionalization on defined P3HT and both polymers were compared. P3HT was synthesized by the Grignard metathesis polymerization (GRIM) developed by McCullough and coworkers.[16] According to the proposed mechanism of GRIM, each polymer chain should bear homogeneously H/Br end groups after polymerization; bromine originating from the starting unit and hydrogen which is formed when quenching the growing chain with hydrochloric acid.[17,18] In fact one usually gets a mixture of the expected H/Br and unexpected H/H end groups. The origin of these H/H end groups is not yet clear and complicates further controlled polymer analogous functionalization of P3HT. To functionalize both chain ends one must find a method that is independent of the nature of the end groups. Therefore, we choose a lithiation reaction which reacts with the bromine as well as with the hydrogen end groups. The regioregular P3HT was treated with secondary butyl lithium, gaseous carbon dioxide and a mixture of hydrochloric acid in methanol to obtain the carboxylated polymer P3HT–COOH (Scheme 1).

Fig. 1a shows the size exclusion chromatography (SEC) traces of P3HT and P3HT–COOH. P3HT has a narrow molecular weight distribution with a polydispersity index (PDI) of 1.15 and a peak molecular weight (M_p) of 5900 g mol^{-1} with respect to polystyrene standards. According to MALDI-TOF MS this corresponds to a number average molecular weight of 3200 g mol^{-1} meaning it has 19 repeating units. Thus the molecular weight of P3HT is usually

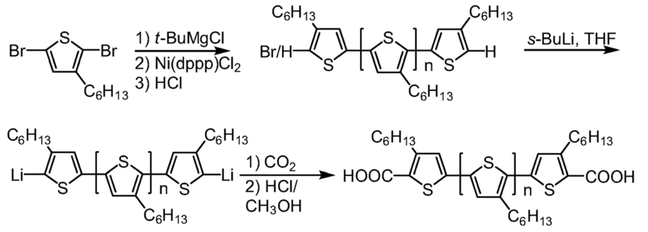

Scheme 1 Synthesis and end group functionalization of regioregular P3HT.

---

[a] *Advanced Functional Polymers, Department of Macromolecular Chemistry I, University of Bayreuth Universitätsstraße 30, 95444 Bayreuth, Germany. E-mail: mukundan.thelakkat@uni-bayreuth.de*
[b] *Institute of Fundamental Studies, Kandy, Sri Lanka*

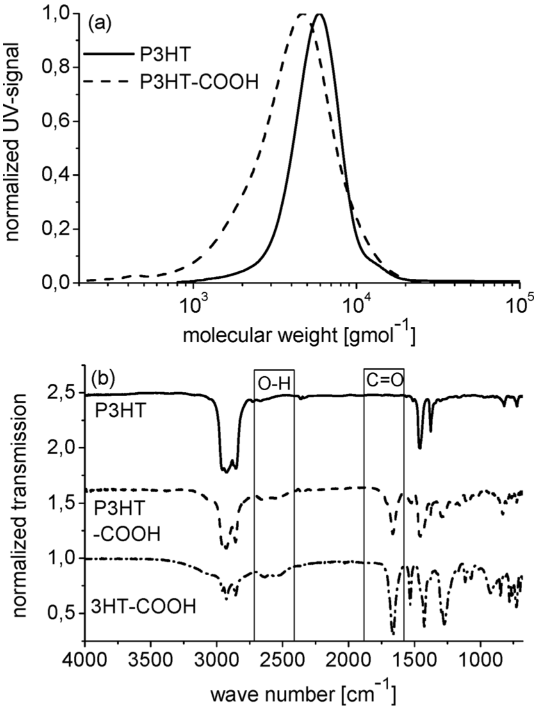

Fig. 1 (a) SEC curves of P3HT (solid) and P3HT–COOH (dashed); (b) FTIR spectra of P3HT (solid) and P3HT–COOH (dashed) in films on a silicon wafer and 3-hexylthiophene-2-carboxylic acid (3HT–COOH) (dash-dotted) as a solid.

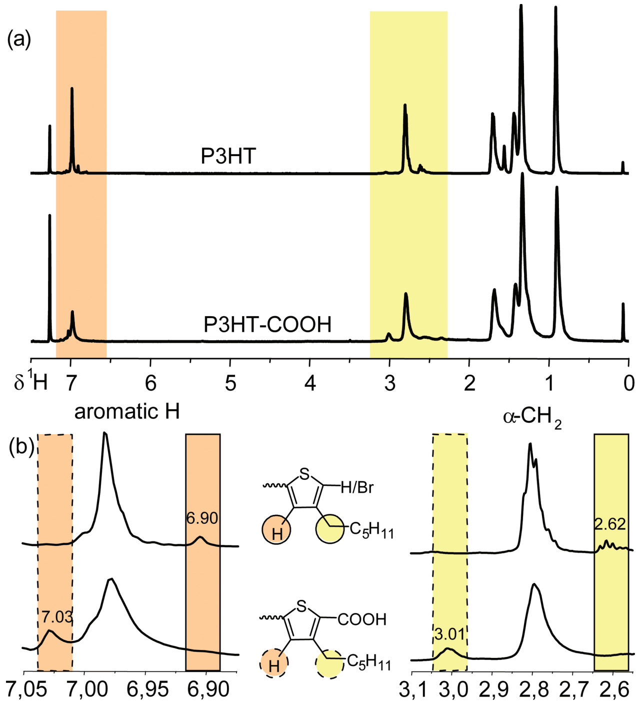

Fig. 2 (a) ^{1}H-NMR spectra of P3HT and P3HT–COOH for comparison measured at 500 MHz. (b) Close up of the aromatic region (left) and the α-CH$_2$ region (right) of the spectra. The rectangles mark the signals belonging to the end group units with the respective COOH or H/Br end groups.

overestimated in SEC if calibrated with polystyrene. The introduction of COOH end groups leads to a broadening of the molecular weight distribution (PDI = 1.68) and a shift of M_p to a lower value of 4700 g mol^{-1} in SEC. Since protic groups tend to interact with the SEC column material, they cause slower elution of P3HT–COOH and broadening of the molecular weight distribution. The monomodal distribution shows that during the ionic functionalization method no chain–chain coupling occurred, a common problem with post-polymerization functionalization of polymers. Additional proof of COOH end groups is given by the FTIR spectrum in Fig. 1b. Compared to the spectrum of P3HT, the P3HT–COOH spectrum has three additional signals; a C=O vibration at 1665 cm^{-1} and O–H vibrations at 2542 cm^{-1} and 2644 cm^{-1}. Moreover, the FTIR bands of the COOH groups are at wave numbers corresponding to hydrogen bonded acid groups. This is further confirmed by comparison with a low molecular weight model molecule, 3-hexylthiophene-2-carboxylic acid (3HT–COOH) (Fig. 1b). While 3-hexylthiophene is a liquid, the introduction of an acid group solidifies 3HT–COOH by building intermolecular hydrogen bonds. Actually, the FTIR signals of the carboxyl group of 3HT–COOH are at the same wave numbers as for the analogous polymer P3HT–COOH. These hydrogen bonds in P3HT–COOH also strongly influence the thermal properties of the polymer. P3HT has a melting point at 174 °C, which is typical for its molecular weight. In contrast P3HT–COOH does not melt before degradation.

Fig. 2 shows ^{1}H-NMR spectra of P3HT and its analogue P3HT–COOH. It is known that different P3HT end groups are visible in the ^{1}H-NMR spectra. The introduction of the COOH groups leads in general to a broadening of the signals for P3HT–COOH which is typical for molecules with hydrogen bonds. In the region of the aromatic protons (Fig. 2b left) both polymers have one main signal at 6.98 ppm. The small signal at 6.90 ppm for P3HT belongs to the end group unit with a hydrogen. In P3HT–COOH this signal vanished but a new signal for the end group unit with a COOH appeared at 7.03 ppm. Changes also occur in the region of the α-CH$_2$ protons. As well as the main signal at 2.80 ppm there are signals at 2.62 ppm (in P3HT) or 3.01 ppm (in P3HT–COOH) belonging to the α-CH$_2$ protons of the respective end group units. These signals are at the same positions as the main α-CH$_2$ signals for the respective low molecular model molecules, 3-hexylthiophene (2.62 ppm) and 3HT–COOH (3.01 ppm). This is possible because the α-CH$_2$ protons are not directly connected to the conjugated system. The analogy shows that low molecular weight model molecules are efficient in identifying diverse end groups in P3HT. An integration of the signals at 2.8 ppm and 3.01 ppm in P3HT–COOH gives quantitative information about the amount of COOH end groups. The integral ratio of these two signals is 17 : 2, which is consistent with a difunctionalized polymer with 19 repeating units as determined by MALDI-TOF MS.

Fig. 3a shows the normalized UV-vis spectra of both polymers measured on thin films (~200 nm) on quartz. While P3HT has vibronic bands typical of π–π stacking, this fine structure is missing in the spectrum of P3HT–COOH. Additionally the maximum absorption (λ_{max}) is significantly hypsochromically shifted from 506 nm in P3HT to 446 nm in P3HT–COOH. The hydrogen bonds in P3HT–COOH can fix the polymer chain in a disordered conformation and thus hinder the π–π stacking. This assumption is also supported by the fact that P3HT–COOH shows no vibronic bands even after annealing. Hydrogen bonds

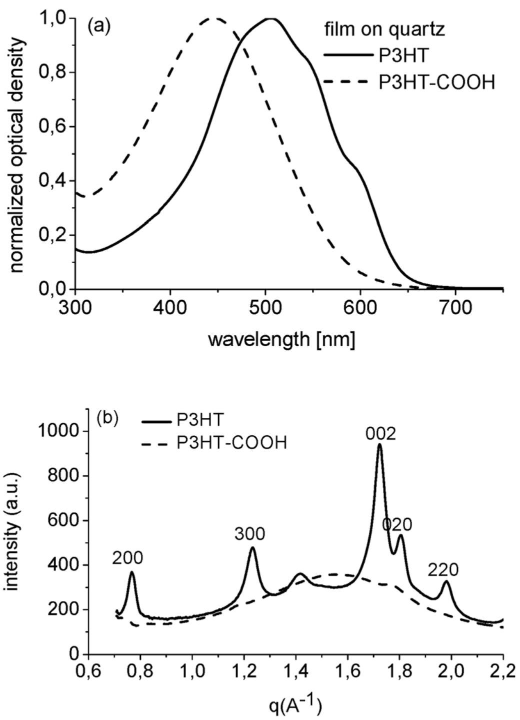

Fig. 3 (a) Normalized UV-vis spectra of P3HT (solid) and P3HT–COOH (dashed) measured on thin films (~200 nm) on quartz. (b) Wide angle X-ray scattering (WAXS) measurements of P3HT (solid) and P3HT–COOH (dashed) in bulk. (*h*00)-Reflections due to lamellar packing of main and side chains, (00*l*)-reflections for the repeating distance of the aromatic rings along the main chain and (020)-reflections for the π–π stacking distance. In comparison to the highly ordered P3HT, P3HT–COOH shows a rather amorphous structure in UV-vis and WAXS measurements.

are thermally stable interactions and hinder the comparatively weaker electrostatic π–π interactions. Thus the missing π–π stacking causes the hypsochromic shift of the λ_{max} and the loss of the fine structure in the UV-vis spectrum. Another contribution to this blueshift of 60 nm is the electron-withdrawing nature of the carboxyl groups.

The missing order is further confirmed by wide angle X-ray diffraction measurements of bulk samples in Fig. 3b. Unfunctionalized P3HT shows typical reflections for regioregular poly(3-hexylthiophene) (*h*00)-reflections due to lamellar packing of main and side chains in the measured range, (00*l*)-reflections for the repeating distance of the aromatic rings along the main chain and (020)-reflections for the π–π stacking distance.[19] In contrast, the diffraction pattern of P3HT–COOH shows an almost completely amorphous structure. Thus the COOH end groups can form a hydrogen bonded network which hinders the typical crystallisation of regioregular P3HT.

Dye-uptake test on mesoporous TiO$_2$

To study the chemisorption of P3HT–COOH on mesoporous TiO$_2$, dye-uptake tests were performed on TiO$_2$ electrodes used for dye-sensitized solar cells. These electrodes consist of mesoporous TiO$_2$ prepared on top of a compact TiO$_2$ layer on FTO (fluorine-doped tin oxide) glass. Solutions (1 wt%) of P3HT and P3HT–COOH in CHCl$_3$ were applied to the substrates. Fig. 4 displays the substrates coated with (a) P3HT and (b) P3HT–COOH before and (c) P3HT and (d) P3HT–COOH after rinsing with chlorobenzene and the respective UV-vis absorption spectra after washing. The difference in color between P3HT (purple) and P3HT–COOH (orange) coated TiO$_2$ substrates can be explained by the difference in the absorption spectra of the two polymers shown in Fig. 3a. It demonstrates that the missing π–π stacking and the hypsochromic shift of the λ_{max} are visible with the naked eye. The UV-vis spectra of the substrates after rinsing (Fig. 4e) demonstrate that only P3HT–COOH chemisorbs on the mesoporous TiO$_2$. The optical density of P3HT–COOH after rinsing is still around 1.5 for λ_{max} while P3HT is removed completely. The reason for the poor spectral quality at low wavelengths is the high UV absorption of the TiO$_2$–FTO substrate.

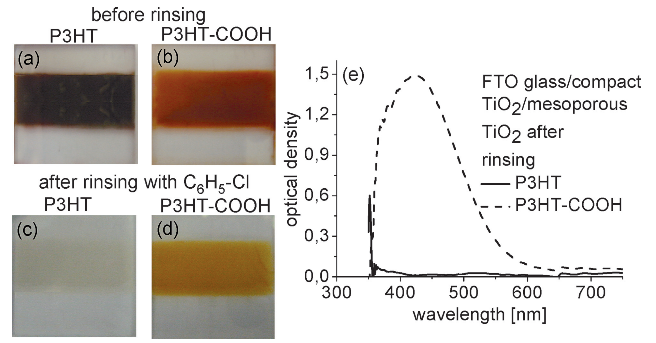

Fig. 4 Pictures of FTO glass/compact TiO$_2$/mesoporous TiO$_2$ coated with (a) P3HT, (b) P3HT–COOH before and (c) P3HT, (d) P3HT–COOH after rinsing with chlorobenzene. (e) UV-vis spectra of P3HT (solid) and P3HT–COOH (dashed) on FTO glass/compact TiO$_2$/mesoporous TiO$_2$ after rinsing with chlorobenzene. Unfunctionalized P3HT is rinsed away completely, while P3HT–COOH still shows an optical density of 1.5 at λ_{max} after rinsing.

Application as a polymer sensitizer

The chemisorption test obviously demonstrates that the COOH groups in end group carboxylated P3HT–COOH are strong enough to anchor onto mesoporous TiO$_2$ and allow its use as a polymer sensitizer in dye-sensitized solar cells. To complete the device preparation, the P3HT–COOH coated mesoporous TiO$_2$ electrode was filled with a solid hole conductor 2,2′,7,7′-tetrakis-(*N*,*N*-di-4-methoxyphenylamino)-9,9′-spiro-bifluorene (spiro-OMeTAD) and finally coated with a Au electrode. To prove that P3HT–COOH does not block the pores and allows filling of the whole mesoporous layer, scanning electron microscopy (SEM) images of the solar cell before and after filling with hole conductor are compared (Fig. 5). From the complete cross-section of such a solid-state cell (Fig. 5a), it is obvious that the hole conductor fills the sensitized film very efficiently even down to the bottom. The comparison of the coated titania and non-coated titania in Fig. 5b and c reveals the same. While in Fig. 5c, bare TiO$_2$ nanocrystals can be observed, the filling with spiro-OMeTAD smooths the edges of the crystals as seen in Fig. 5b. Since the image of the filled mesoporous TiO$_2$ layer in Fig. 5b is from the bottom of the solar cell, it proves that

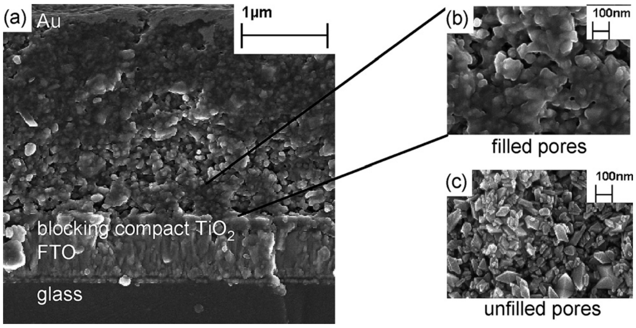

Fig. 5 (a) SEM image of the solar cell consisting of FTO glass/compact TiO_2/mesoporous TiO_2/P3HT–COOH/spiro-OMeTAD/Au. (b) Magnification of the bottom part of the mesoporous TiO_2 layer filled with P3HT–COOH and spiro-OMeTAD. (c) SEM image of bare TiO_2 nanocrystals. Comparison of (b) and (c) proves that there is a deep infiltration of the hole conductor even down to the bottom most part of the active layer.

there is a deep infiltration. It can also be seen in the SEM image (Fig. 5a) that there is a very thin over standing layer of the solid hole conductor (spiro-OMeTAD) on top, which helps to avoid any shorting between the titania and top electrode.

Fig. 6a shows a schematic representation of the device architecture and the current–voltage characteristics of the solar cell measured under AM 1.5 spectral conditions and under sunlight intensity. P3HT–COOH as a polymer sensitizer allows a better surface coverage of TiO_2, thus helping to avoid any recombination between the titania and hole conductor. Additionally, P3HT chains can also act as a hole conductor and thus contribute to charge transport. However these complementary functions could not be differentiated here in the first test results. The device with a P3HT–COOH as a polymer sensitizer shows good current–voltage characteristics in the dark and under illumination (Fig. 6b). A typical behavior of a photodiode without a current up to an open circuit voltage of 0.54 V is indicated by the dark current (dashed line). The short-circuit current is 3.7 mA cm^{-2}, the fill factor is 46% and the efficiency is 0.9%. These are very promising values for a polymer sensitized solid-state device.

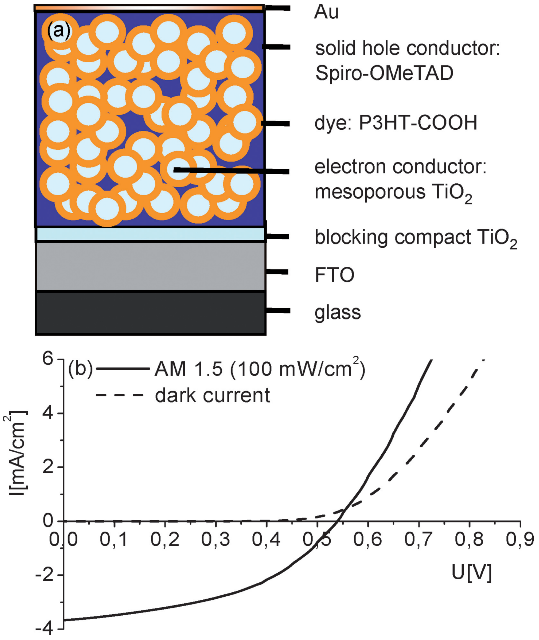

Fig. 6 (a) Device structure of the solar cell as a schematic. (b) Current–voltage characteristic of the solar cell in dark (dashed) and under illumination (solid) at AM 1.5 at 100 mW cm^{-2}. Typical values are: open circuit voltage = 0.54 V, short-circuit current = 3.7 mA cm^{-2}, fill factor = 46% and power conversion efficiency = 0.9%.

Conclusion

In conclusion, P3HT with COOH end groups was synthesized and its chemisorption on mesoporous TiO_2 was studied. The solar cells prepared with P3HT–COOH as a sensitizer and spiro-OMeTAD as a solid hole conductor showed a good efficiency of 0.9%. This is promising because the absorption of P3HT can be tuned by introducing different side chain substituents. Adjusting the chain length is also a method to improve the absorption, charge transport mobility and the performance of the solar cell.[20,21] Since P3HT–COOH can also act as a hole conductor, this may enable the construction of solar cells with one component fulfilling both functions of sensitization and hole transport. Previously we have shown that dyes, carrying polymeric donor groups, can also retard recombination in a highly efficient way.[22] It is not yet clear if this is also the case for P3HT–COOH. Therefore, detailed studies of transfer and recombination dynamics with time-resolved absorption spectroscopy are under investigation.

Experimental

General information

^{1}H-NMR spectra were recorded in chloroform on a Bruker DRX 500 spectrometer at 500 MHz. Coupling constants are given in Hz. SEC measurements were carried out in THF using a UV detector from Waters and a mixed-C PL-Gel (PL) column. Polystyrene was used as external standard and 1,2-dichlorobenzene as an internal standard for calibration. FTIR spectra were obtained from drop-cast films on silicon wafers with a BIO-RAD Digilab FTS-40. UV-vis measurements were performed with a U-3000 spectrometer from Hitachi. X-Ray measurements were made at the DUBBLE beamline ID 26 at ESRF in Grenoble. The used wavelength was 1.0415 Å and wide angle X-ray data were collected with a microstrip gas chamber detector. The monomer 2,5-dibromo-3-hexylthiophene and the catalyst 1,3-bis(diphenylphosphino)propanenickel(II) chloride [Ni(dppp)Cl_2] were synthesized according to the literature.[23,24] All glass apparatus for polymerization and polymer-analogous reactions were baked out and cooled down under argon. Dry THF was distilled over calcium hydride and potassium. Tertiary butyl magnesium chloride 2.0 M in THF was purchased from Fluka and titrated according to Krasovskiy and Knochel.[25] Secondary butyl lithium [1.3 M solution in cyclohexane–hexane (Acros)] and CO_2 gas (99.995% <5 ppm H_2O, Rießner Gase) were used as received.

Solar cell preparation and characterization

The solar cells were prepared according to Karthikeyan and Thelakkat with nanocrystalline-titanium dioxide pastes from Energy Research Center (ECN), Netherlands.[5] The hole conductor used was a mixture of spiro-OMeTAD, $Li(CF_3SO_2)_2N$ and *tert*-butylpyridine (tbp) in an optimized composition.[5] The *I*–*V* characterization was carried out using a calibrated xenon lamp with suitable filters to obtain AM 1.5 spectral irradiation and an intensity of 100 mW cm^{-2}. The lamp was regularly calibrated with ISE Call lab, Freiburg silicon solar cell (WPVS cell). The *I*–*V* values were recorded using a Keithley 6517 source measure unit.

Synthesis of P3HT

P3HT was synthesized according to published procedures.[13] The polymer was used without purification by fractionation and yielded 2.25 g (70%) of a purple powder. GPC $M_p = 5900$ g mol^{-1}, $M_n = 5200$ g mol^{-1}, $M_w = 6000$ g mol^{-1}, $M_w/M_n = 1.15$; MALDI-TOF MS $M_n = 3200$ g mol^{-1}, $M_w = 3400$ g mol^{-1}, $M_w/M_n = 1.15$; δ_H (500 MHz; $CDCl_3$) 6.98 (1 H, s, H_{ar}), 6.90 (1 H, s, H_{ar} of end group unit with H end group), 2.80 (2 H, t, $J_{\alpha\beta}$ 7.6, α-CH_2), 2.62 (2 H, t, α-CH_2 of end group unit with hydrogen), 1.85–1.50 (2 H, m, β-CH_2), 1.50–1.10 (6 H, m), 1.0–0.75 (3 H, m, CH_3); FTIR ν_{max}(film)/cm^{-1} 3056w, 2955s, 2927s, 2857s, 1512w, 1456m, 1378m, 821m, 726w. UV-vis λ_{max}(film)/nm 506.

Synthesis of P3HT–COOH

P3HT (566 mg, $M_n = 5200$ g mol^{-1}) was dried under vacuum and dissolved in dry THF (243 mL). The solution was cooled down to −78 °C and secondary butyl lithium in hexane (2.3 mL, 2.99 mmol) was added in one portion. After 1 h of stirring the solution was heated to 40 °C for 20 min to inactivate excess *s*-BuLi. The solution was cooled down to −78 °C again and gaseous CO_2 was introduced for 1 h. After 30 min of additional stirring, the reaction was terminated with a mixture of HCl and methanol (v : v, 1 : 9). The functional polymer was filtered, washed with methanol and extracted with chloroform. Pure P3HT–COOH (576 mg) was isolated from the chloroform extract by precipitation into methanol, filtering and drying under vacuum. GPC $M_p = 4700$ g mol^{-1}, $M_n = 2800$ g mol^{-1}, $M_w = 4700$ g mol^{-1}, $M_w/M_n = 1.68$. δ_H (500 MHz; $CDCl_3$) 7.03 (1 H, s, H_{ar} of end group unit with COOH), 6.98 (1 H, br s, H_{ar}), 3.01 (2 H, t, α-CH_2 of end group unit with COOH), 2.80 (2 H, br, α-CH_2), 1.85–1.50 (2 H, br m, β-CH_2), 1.50–1.10 (6 H, br m), 1.0–0.75 (3 H, br m, CH_3); FTIR ν_{max}(film)/cm^{-1} 3055w, 2957s, 2928s, 2857s, 2644b, 2542b, 1665s, 1526w, 1457s, 1439s, 1378w, 829m, 724w. UV-vis λ_{max}(film)/nm 446.

Acknowledgements

We acknowledge financial support for this research work from DFG SPP 1355 and Eurocores-Sons-II (SOHYDs). J. Bandara thanks the AvH foundation for stipend. R. H. Lohwasser thanks the elite network Bavaria for financial support. Further we acknowledge the European Synchrotron Radiation Facility for the ID26–DUBBLE–Dutch-Belgian beamline. Special thanks go to Christian Müller from Linköpings University for his support at the beamline and for evaluation of the X-ray data.

References

1 M. Grätzel, *Prog. Photovoltaics*, 2006, **14**, 442.
2 M. Grätzel, *Nature*, 2001, **414**, 338.
3 U. Bach, D. Lupo, P. Comte, J. E. Moser, F. Weissörtel, J. Salbeck, H. Spreitzer and M. Grätzel, *Nature*, 1998, **395**, 583.
4 J. Hagen, W. Schaffrath, P. Otschik, R. Fink, A. Bacher, H. W. Schmidt and D. Haarer, *Synth. Met.*, 1997, **89**, 215.
5 C. S. Karthikeyan and M. Thelakkat, *Inorg. Chim. Acta*, 2008, **361**, 635.
6 K. Tennakone, V. P. S. Perera, I. R. M. Kottegoda and G. R. R. A. Kumara, *J. Phys. D: Appl. Phys.*, 1999, **32**, 374.
7 J. Yum, D. P. Hagberg, S. Moon, K. M. Karlsson, T. Marinado, L. Sun, A. Hagfeldt, M. K. Nazeeruddin and M. Grätzel, *Angew. Chem., Int. Ed.*, 2009, **48**, 1576.
8 G. K. R. Senadeera, K. Nakamura, T. Kitamura, Y. Wada and S. Yanagida, *Appl. Phys. Lett.*, 2003, **83**, 5470.
9 G. K. R. Senadeera, T. Kitamura, Y. Wada and S. Yanagida, *Sol. Energy Mater. Sol. Cells*, 2005, **88**, 315.
10 K. Shankar, G. K. Mor, H. E. Prakasam, O. K. Varghese and C. A. Grimes, *Langmuir*, 2007, **23**, 12445.
11 S. Yanagida, G. K. R. Senadeera, K. Nakamura, T. Kitamura and Y. Wada, *J. Photochem. Photobiol., A: Chem.*, 2004, **166**, 75.
12 H. Sirringhaus, N. Tessler and R. H. Friend, *Science*, 1998, **280**, 1744.
13 M. Jeffries-El, G. Sauve and R. D. McCullough, *Macromolecules*, 2005, **38**, 10346.
14 B. M. W. Langeveld-Voss, R. A. J. Janssen, A. J. H. Spiering, J. L. J. Van Dongen, E. C. Vonk and H. A. Claessens, *Chem. Commun.*, 2000, 81.
15 J. Liu and R. D. McCullough, *Macromolecules*, 2002, **35**, 9882.
16 R. S. Loewe, P. C. Ewbank, J. Liu, L. Zhai and R. D. McCullough, *Macromolecules*, 2001, **34**, 4324.
17 R. Miyakoshi, A. Yokoyama and T. Yokozawa, *J. Am. Chem. Soc.*, 2005, **127**, 17542.
18 E. E. Sheina, J. Liu, M. C. Iovu, D. W. Laird and R. D. McCullough, *Macromolecules*, 2004, **37**, 3526.
19 S. Hugger, R. Thomann, T. Heinzel and T. Thurn-Albrecht, *Colloid Polym. Sci.*, 2004, **282**, 932.
20 R. J. Kline, M. D. McGehee, E. N. Kadnikova, J. Liu and J. M. J. Frechet, *Adv. Mater.*, 2003, **15**, 1519.
21 W. Ma, J. Y. Kim, K. Lee and A. J. Heeger, *Macromol. Rapid Commun.*, 2007, **28**, 1776.
22 S. A. Haque, S. Hana, K. Peter, E. Palomares, M. Thelakkat and J. R. Durrant, *Angew. Chem., Int. Ed.*, 2005, **44**, 5744.
23 R. S. Loewe, M. S. Khersonsky and R. D. McCullough, *Adv. Mater.*, 1999, **11**, 250.
24 G. R. Van Hecke and W. Horrocks, *Inorg. Chem.*, 1966, **5**, 1968.
25 A. Krasovskiy and P. Knochel, *Synthesis*, 2006, **5**, 890.